Advanced Photon Source Activity Report for 2003: Bubble Size Distributions in Silicate Foams Measured by X-ray Microtomography

D.R. Baker[1], G. Robert[1], M.L. Rivers[2], E. Allard[1], J. Larocque[1]
[1]Earth and Planetary Sciences, McGill University, Montréal, QC CANADA
[2]GSE CARS and Department of Geophysical Sciences, University of Chicago, Chicago, IL USA

INTRODUCTION

Bubbles and foams are ever present in our daily lives: they are found in the insulation that protects our homes from climate extremes, they often cushion the seats upon which we sit, they help us wash our clothes, and they are in the bread we eat and the beer we may drink. Bubbles also play a significant role in geological processes. As magma, molten rock plus crystals and dissolved volatiles (dominantly H_2O), ascends from depth in the Earth where it was formed by partial melting, the drop in pressure results in the exsolution of a gas phase and the growth of bubbles. Given a sufficient supply of volatiles the magma can develop into a foam whose bubble walls are composed of silicate glass. The exsolution of bubbles can take only a few seconds and is the driving force behind volcanic eruptions. The most violent volcanic eruptions can produce 1000's of cubic kilometers of silicate foams, which are often broken apart by the expansion of the gas to create volcanic ash[1]. This causal connection between bubble formation and volcanic eruptions inspired us to investigate the formation and growth of bubbles in silicate melts with the aim of attaining a better understanding of volcanic eruption processes and the hope that this knowledge will eventually aid in the prediction of devastating volcanic eruptions.

Most previous research on foamed natural and synthetic volcanic rocks measured bubble sizes and densities using two-dimensional images[2-6] and converted these results into three dimensions using stereological formulas [7]. Although one study utilized microtomography to investigate the bubble size distribution in basaltic rocks[8], no one has systematically compared bubble size distributions obtained in two-dimensional sections with tomographic reconstructions. Because the bubbles in these samples are not simple, convex spheres, but more complexly shaped volumes, there may be inaccuracies introduced by the conversion of two-dimensional measurements into three dimensions. These inaccuracies might invalidate the conclusions reached in previous research based upon two-dimensional image analysis. The goal of our research was to use x-ray microtomography to compare the bubble size distribution measured from two-dimensional x-ray slices with the completely reconstructed tomographic image of the sample.

Measurement of the bubble size distribution formed by the exsolution of a gas from a liquid is an excellent test for the comparison of two-dimensional and three-dimensional imaging techniques. Many of the previous two-dimensional studies found that bubble size distributions follow a power law and there exist at least three theories that predict the value of the power law exponent for the distribution of bubble volumes [6, 9, 10]; the theories agree in their prediction that the power law exponent for the cumulative bubble volume is 1. Thus, we not only compare the bubble size distributions measured in two and in three dimensions with each other, but we can also make the comparison between the exponent predicted by theory and the experimentally determined distribution.

METHODS AND MATERIALS

We synthesized two hydrated glasses; the first, AB24, was albitic in composition ($NaAlSi_2O_8$) and represents rhyolitic volcanic melts. The second, SB4, was made from a natural basalt from the island of Stromboli, Italy, which was investigated because basalts are the dominant form of volcanic rock on the Earth and because of the violent eruption that occurred at Stromboli on April 5, 2003. We hydrated AB24 with 10.9 wt % H_2O and SB4 with 5 wt % H_2O; we performed sample hydration by melting the glass + water mixtures in a piston cylinder apparatus using crushable alumina-Pyrex-NaCl assemblies at 1100 ºC and 550 MPa for one hour followed by isobaric quenching to glass in less than 20 s. This procedure produced homogeneously hydrated glasses containing no crystals. We foamed SB4 in the laboratory by heating it to 1050 °C in a miniature furnace. This glass foam was mounted on a toothpick for x-ray microtomography. Sample AB24 was degassed at approximately 750 °C directly on the beamline used for microtomography, BM-13 of GSECARS at the Advanced Photon Source, in a custom-designed boron-nitride furnace (Fig. 1). The furnace is split in half along the horizontal plane defined by the pedestal upon which the sample sits and during tomography the top half of the furnace can be removed for tomography. Tomography was performed by collecting x-ray images during 180 degrees rotation; the sample was rotated at ¼ degree resolution resulting in the collection of a total of 720 images [11]. Transmitted x-rays were converted into visible light with a YAG phosphor screen that was imaged with either a 5x or a 10x objective and a cooled a CCD camera with a spacing of 13.4 μm/pixel and with a binning of 2x2. We were able to achieve spatial resolutions ranging from 3.85 μm/pixel to 6.63 μm/pixel by changing the objective lens and the focal length between the lens and the CCD camera. The beam energies necessary for our data collection were between 15 and 20 KeV and counting times varied from 2.5 to 1.5 s per angular step. Reconstruction of the tomographic images was performed using the Gridrec Fourier Transform algorithm producing 512 two-dimensional image slices, which together produce the three-dimensional reconstruction of the sample. These images demonstrated that the bubbles in our foamed samples were not simple spheres, but complexly shaped bodies due to the coalescence of multiple bubbles.

Because our goal was to compare bubble size distributions measured in two dimensions with those measured in three, we analyzed two-dimensional image slices of the sample. For this analysis we selected a minimum of six image slices from near the center of the sample and used the software ImageJ (http://rsb.info.nih.gov/nih-image/). The smallest bubble we could image was on the order of 100 μm^2, or 3 x 3 pixels. Bubbles were segmented by gray-scale thresholding followed by removal of "holes" and "islands" and their two-dimensional areas were counted.

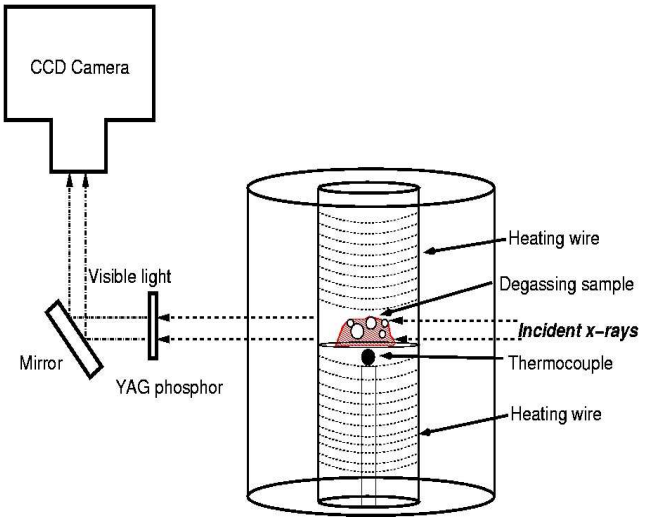

Fig. 1. Schematic of furnace used for sample foaming and tomography (not to scale; the outer diameter of the furnace is 19 mm).

We performed three-dimensional analysis with the software package BLOB3D written by Richard Ketcham of the University of Texas. The smallest bubble we could image was on the order of 1000 μm^3, which corresponds to 3 x 3 x 3 voxels. The blobs in the image, which represent the bubbles in the sample, were segmented based upon gray scale thresholding followed by "hole" and "island" removal. Importantly, we used no other type of filter or transformation during the segmentation process. Large, complexly shaped blobs were eroded by removing 1 pixel from the surface, which often produced multiple sub-blobs which were then dilated back by addition of the surface pixels removed in the erosion step to produce a collection of small sub-blobs. Often after dilation the surfaces of many blobs touched each other. This behavior implies that two separate bubbles exist in the sample, but that these bubbles have no septum of glass separating them; such a state is impossible and in every two dimensional image slice we observed glass septa between the bubbles with a minimum thickness of at least 1 pixel. To separate large complex blobs into sub-blobs which were separated by septa of at least voxel in thickness we first eroded the large blob into sub-blobs and then dilated, thus producing many small blobs sharing surfaces. After dilation, the small blobs with flat faces were eliminated, either by postponing if they were on the edge of the segmented volume investigated or deleting if they were in the center of the volume and had flat edges. After removal of these anomalous blobs we reconnected all blobs whose surfaces touched into larger blobs, typically producing 1 large blob and a few small blobs in the investigated volume.

After all bubble areas or volumes were counted in either two- or three-dimensions (respectively), the cumulative distribution of the bubble areas and volumes was plotted to determine the type of distribution (e.g., unimodal, multimodal, exponential, power-law) for comparison with theory. The bubble sizes for the larger bubbles in each sample follow power law distributions whose exponents were determined from the slopes on the cumulative distribution plots; uncertainties in these slopes are difficult to estimate, but previous researchers [5] suggest that we can expect uncertainties of approximately 0.3.

RESULTS AND DISCUSSION

The cumulative distribution of bubble sizes in AB24 for the 2-dimensional area and 3-dimensional volume measurements are shown in Fig. 2. For sample SB4 the corresponding 2-dimensional and 3-dimensional measurements are shown in Fig. 3. The bubble sizes in AB24 display a power distribution in both 2- and 3-dimensional measurements; in both cases the value of the exponent is close to 1. Analysis of 2-dimensional bubble areas in sample SB4 produced a power law distribution with an exponent of approximately 1; the three-dimensional SB4 bubble volumes are also power-law distributed, but with an exponent of approximately 1.4.

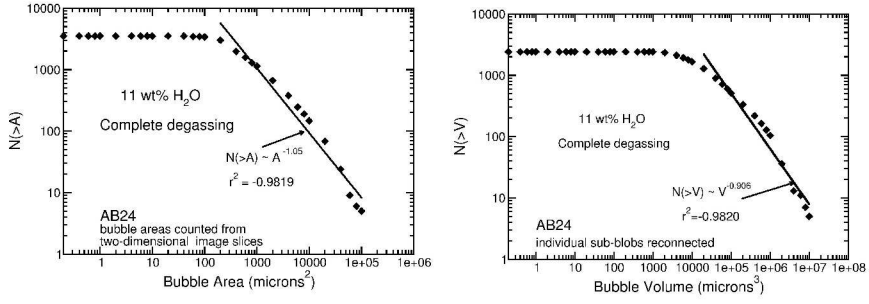

Fig. 2 Cumulative bubble area and volume distributions for AB24

Given that the probability of measuring a bubble with an area greater than A, or P(>A), is proportional to A^{-n}, and that probability theory requires that P(A)dA = P(V)dV, where V is the bubble volume, we can use our two dimensional area distributions to calculate the exponents of the three dimensional volume distributions. Using the power-law exponents presented in the figures we can perform this analysis. To begin we convert the cumulative distributions into non-cumulative ones through differentiation. The next step is to convert areas into radii and then convert the radii from two into three dimensions [6]. These radii are easily converted into three-dimensional bubble volumes and the result is that $P(>V) \quad V^{-(2n/3+1/3)}$ [5,6,9]. This conversion demonstrates that the two-dimensional measurements for sample AB24 accurately represent the true, three-dimensional bubble volume distribution. The difference we find between the calculated and measured volume exponent for SB4 is slightly greater than our estimated uncertainty. We think the discrepancy is due to over-counting of the largest bubbles in the two dimensional image slices. Only if the 2-dimensional cumulative area exponent is increased to 1.6, far above the sum of our measured cumulative area exponent and our estimated uncertainty, can the calculated and measured volume exponents become consistent. At the present we can offer no explanation of the difference we find, other than the suggestion that the few two-dimensional slices we investigated

were not statistically representative of the whole foam. The difference between the estimated and measured bubble volume exponent for this sample demonstrates the utility of microtomography in accurately measuring bubbles in foams.

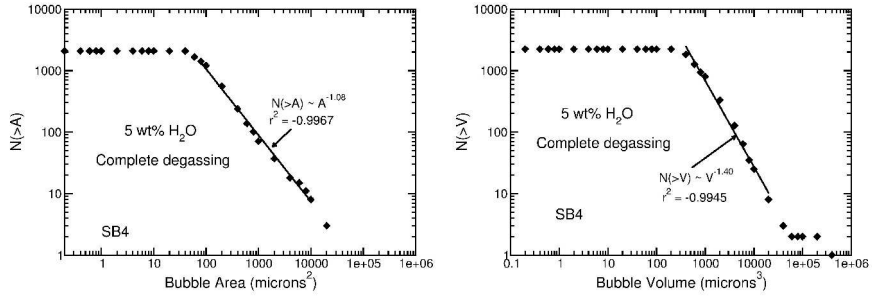

Fig. 3 Cumulative bubble area and volume distributions for SB4

The bubble volume distributions we measured can be compared against theories for bubble growth, for aggregation, and for random packing of spheres. Gaonac'h et al. [5,9] present a model for predicting the value of the cumulative bubble volume exponent; by applying a binary coalescence model to explain large bubbles, they find that the cumulative volume exponent is 1 [9]. Comparison of theory and studies of natural rocks demonstrated close agreement between theory and measurement [5]. However, other models of bubble growth and coagulation also exist to explain the bubble size distribution. Buldyrev et al. [10] discussed an aggregation model that explains the power-law distribution of objects in a "basin of attraction" consisting of many hierarchical levels. Application of this model to bubble growth implies that a bubble growing in a larger basin of attraction is larger than a bubble growing in a smaller basin and that the power law describing the cumulative volume distribution resulting from this model has an exponent of 1. Finally, because the experimental foams approach the limit for packing random objects (Fig. 2), one more model for consideration is that of packing-limited growth, in which randomly sized spheres are placed into a volume; the resulting power-law distribution of sphere sizes indicates a cumulative volume exponent also of approximately 1 [12]. All of the above models predict cumulative volume distribution exponents near 1. Our measurements of sample AB24 agree, within uncertainty, with all these theories. On one hand this agreement is excellent, it supports the validity of the bubble size distribution measurements in both two and three dimensions for this sample, but unfortunately we cannot distinguish between the different growth mechanims of the various theories. Although at first consideration the exponent for SB4, 1.4, does not seem significantly higher than those measured for AB24, comparison with the theories briefly described above highlights the anomalous nature of the bubble size distribution measured in SB4. Our results suggest that melt composition has an effect on the bubble volume distribution. Although we cannot definitively explain the source of this higher exponent at this time, we can speculate that the different behavior of SB4 is related to its lower anhydrous viscosity at the foaming conditions. Our study demonstrates the utility of x-ray microtomography as a tool for the study of the bubble size distribution in silicate foams made by heating hydrated glasses at 1 atmosphere pressure. Analysis of the bubbles requires careful attention because of the possibility of accidentally identifying separate bubbles (blobs) with large areas of touching interfaces, which are physically implausible. Comparison of cumulative bubble area measurements made on a few image slices with the complete cumulative bubble volume measurements made on the three-dimensional image indicates that in some cases two-dimensional measurements yield accurate values of the power-law exponents, but in other cases they do not. We attribute these differences in SB4 primarily to the complex shapes of the bubbles in our samples (only the small ones are spherical) and to the limited number of two-dimensional slices we used to measure the bubble area distribution. Comparison of our measured distributions with theories of bubble growth demonstrate agreement for AB24 but not for SB4, which displays an enigmatically large cumulative bubble volume exponent.

ACKNOWLEDGMENTS

We thank all of the scientists and support staff at GSECARS and the Advanced Photon source for their work in keeping the beam lines and the synchrotron operating at peak performance. We thank Mr. Steve Kecani, Department of Physics, McGill University, who helped design and who fabricated the furnaces we used on this project. GeoSoilEnviroCARS is supported by the National Science Foundation - Earth Sciences (EAR-0217473), Department of Energy - Geosciences (DE-FG02-94ER14466) and the State of Illinois. Use of the Advanced Photon Source was supported by the U.S. Department of Energy, Office of Science, Office of Basic Energy Sciences, under Contract No. W-31-109-ENG-38. This research was partially funded by an NSERC Discovery grant to D.R. Baker.

REFERENCES

1. R.S.J. Sparks, J. Barclay, C. Jaupart, H.M. Mader, J.C. Phillips, in: *Rev. Mineral.*, **30,** 413-445, Min. Soc. Am. (1994).
2. A. Toramaru , J. Geophys. Res. **94**, 17523-17542, (1989).
3. A. Toramaru, J. Volcan. Geotherm. Res. **43,** 71-90 (1990).
4. K.V. Cashman, M.T. Mangan, in: *Rev. Mineral.* **30,** 447-478, Min. Soc. Am. (1994).
5. H. Gaonac'h, J. Stix, S. Lovejoy, J. Geophys. Res. **74**, 131-153 (1996).
6. J.D. Blower, J.P. Keating, H.M. Mader, J.C. Phillips, J. Volcan. Geotherm. Res. **120,** 1-23 (2002).
7. D.L. Sahagian, A.A. Proussevitch J. Volcan. Geotherm. Res. **84**, 173-196 (1998).
8. S.-R. Song, K.W. Jones, W.B. Lindquist, B.A. Dowd, D.L. Sahagian. Bull. Volcan. **63**, 252-263 (2001).
9. H. Gaonac'h, S. Lovejoy, J. Stix, J., D. Scherzter, Earth Planet. Sci. Lett. **139**, 395-409 (1996).
10. S.V. Buldyrev, N.V. Dokholyan, S. Erramilli, M. Hong, J.Y. Kim, G. Malescio, H.E. Stanley, Physica A **330**, 653-659 (2003).
11. M.L. Rivers, S.R. Sutton, P. Eng, Proceedings of SPIE, Developments in X-Ray Tomography II **3772**, 78-86 (1999).
12. P.S. Dodds, J.S. Weitz, *Phys. Rev. E* **65**, 056108 (2002).